Sains Malaysiana 54(8)(2025): 2045-2057
http://doi.org/10.17576/jsm-2025-5408-14

Microstructural Evolution and Performance of Heat-Treated Ti6Al4V in Laser Powder Bed Fusion

(Evolusi Mikrostruktur dan Prestasi Ti6Al4V Haba Terawat Haba dalam Pelakuran Lapisan Serbuk Laser)

FARHANA MOHD FOUDZI[1,2,*], MINHALINA AHMAD BUHAIRI[1,2,3], FATHIN ILIANA JAMHARI[1,2], NORHAMIDI MUHAMAD[1,2], INTAN FADHLINA MOHAMED[1,2], ABU BAKAR SULONG[1,2], NASHRAH HANI JAMADON[1,2] & NABILAH AFIQAH MOHD RADZUAN[1,2]

[1]*Advanced Manufacturing Research Group, Universiti Kebangsaan Malaysia, 43600 UKM Bangi, Selangor, Malaysia*
[2]*Department of Mechanical and Manufacturing Engineering, Faculty of Engineering and Built Environment, Universiti Kebangsaan Malaysia, 43600 UKM Bangi, Selangor, Malaysia*
[3]*Doctoral School on Materials Science and Technologies, Óbuda University, Nepszinhaz u. 8, 1081 Budapest, Hungary*

Received: 21 February 2025/Accepted: 16 June 2025

ABSTRACT

Ti6Al4V parts produced via laser powder bed fusion (LPBF) frequently exhibit high residual stress, where heat treatment has been utilized to relieve this stress. This study aims to investigate the effect of annealing heat treatment on the overall performance of Ti6Al4V fabricated using LPBF. Printed Ti6Al4V samples were heat treated at 935 °C for 8 h with a heating rate of 5 °C/min and a cooling rate of 0.60 °C/min. The overall performance such as physical properties, mechanical properties and microstructure observation between as-built and heat-treated samples were compared. The heat treatment was able to produce high-density parts, with surfaces as smooth as 5.70 µm, reaching up to 99.28% density. The annealing process significantly improved the ductility of Ti6Al4V parts by up to 231%, while decreasing the tensile strength by 28% and the hardness by 13%. The microstructure of as-built samples shifts from acicular α' martensite to α+β phases after annealing at 935 °C for 8 hours, supporting the changes in mechanical performance. This preliminary study concludes that the heat treatment used following LPBF printing can create Ti6Al4V samples with acceptable physical, mechanical, and microstructure properties.

Keywords: Hardness; heat treatment; laser powder bed fusion; microstructure; Ti6Al4V

ABSTRAK

Produk Ti6Al4V yang dihasilkan melalui kaedah pelakuran lapisan serbuk laser (LPBF) kebiasaannya menjana tegasan baki yang tinggi dengan rawatan haba digunakan untuk mengurangkan tegasan ini. Penyelidikan ini bertujuan untuk mengkaji kesan rawatan haba penyepuhlindapan ke atas prestasi keseluruhan produk Ti6Al4V yang dihasilkan menggunakan LPBF. Sampel Ti6Al4V telah dirawat haba pada 935 °C selama 8 jam menggunakan kadar pemanasan sebanyak 5 °C/min dan kadar penyejukan sebanyak 0.60 °C/min. Prestasi keseluruhan merangkumi sifat fizikal, sifat mekanikal dan analisis mikrostruktur antara sampel sebelum dan selepas dirawat haba telah dibandingkan. Rawatan haba yang telah dijalankan mampu menghasilkan sampel berketumpatan setinggi 99.28% dengan permukaan selicin 5.70 µm. Proses penyepuhlindapan ini juga berjaya meningkatkan kemuluran sampel Ti6Al4V sebanyak 231%, namun proses ini mengurangkan kekuatan tegangan sebanyak 28% dan kekerasan sebanyak 13%. Mikrostruktur sampel yang telah dicetak 3D berubah daripada jejarum α' martensit kepada fasa campuran α+β selepas dirawat haba pada 935 °C selama 8 jam dan ini menyokong perubahan sifat mekanikal. Kajian awal ini menyimpulkan bahawa rawatan haba yang digunakan selepas percetakan LPBF mampu menghasilkan sampel Ti6Al4V dengan sifat fizikal, mekanikal dan mikrostruktur yang boleh diterima.

Kata kunci: Kekerasan; mikrostruktur; pelakuran lapisan serbuk laser; rawatan haba; Ti6Al4V

INTRODUCTION

Laser powder bed fusion (LPBF) process uses laser beam to melt and fuse layers of metallic powders to produce 3D parts. The quick cyclic nature of heating and cooling actions during process causes as-built printed parts to have a significant thermal gradient. This complicated thermal process promotes the formation of residual stress in the solidified powder layers. If residual stress is not considered at the product design stage, it may become a significant contributing cause in product failure. This is

particularly true for intermittent load applications and corrosive settings (Fathin Iliana et al. 2023a; Korkmaz et al. 2022; Mazeeva et al. 2024). Untreated printed parts with high residual stress may also have issues with parts geometry like delamination and warping, in which can be problematic when precise dimensional tolerances are needed. Typically, residual stress is treated using heat treatments such as hot isostatic pressure (HIP) or annealing. The use of such post-printing treatments will have an impact on the microstructure and mechanical performance of the final 3D-printed object.

Figure 1 shows the phase diagram of Ti6Al4V alloy by Majumdar et al. (2019). At room temperature, the Ti6Al4V alloy contains two phases (α+β). Aluminium helps stabilise the α phase, while vanadium helps stabilise the β phase. LPBF's rapid heating, melting, and cooling rates allow for the production of several Ti6Al4V phases, including α, α', and β martensite. During the intense melting of Ti6Al4V alloy, the α+β phase will transform into β phase before becoming liquid. The liquid phase will then transition into β phase during cooling. Consequently, depending on the rate of cooling, the phase may either return to the α+β phase or transition to the α phase. A numerical modelling done by Lee et al. (2024), has detailed the allotropic transformation of these phases according to their temperature region. β-phases begin to nucleate and grow at high temperature above ~980 °C, while lower temperature encourages the transformation of β-phases into α-phase seed, producing a final microstructure of α + β phase at room temperature. Meanwhile α' is a metastable phase that develops when Ti6Al4V is cooled rapidly from α+β region. Narasimharaju et al. (2022) found that the microstructure of LPBF products is finer than conventionally produced parts due to the extreme cooling rate of LPBF at the rate of 10^3-10^8 K/s as supported by Bartolomeu et al. (2022). Wang et al. (2022) suggest that lowering the thickness of the powder layer can result in finer β grains.

Figure 2 shows the microstructure of LPBF Ti6Al4V products, including β grain and four forms of martensite α'. Previous research has identified four types of α' martensite depending on grain size: primary, secondary, tertiary, and quaternary (Pal et al. 2024). The largest α' martensite is known as primary α' martensite, whereas the finest martensite is quaternary α' martensite. Abd-Elaziem et al. (2022) found that high laser power causes several heating and cooling cycles in the powder layers. This will produce dendritic grains perpendicular to the powder layers. Martensite improves Ti6Al4V corrosion resistance and enhances ductility with its continuous β grain structure. Post-processing, such as heat treatment, is necessary to convert the α' martensite phase to the α+β phase and eliminate residual stress from the LPBF process.

Table 1 displays the temperature range of heat treatment and the time required for residual stress reduction. Data from previous investigations have shown that heat treatment is effective in alleviating residual stress. Kruth et al. (2012) observed that a heating temperature of 550 °C can reduce residual stress by 80%, while Leuders et al. (2013) reported an 84.40% reduction for temperatures ranging from 750 °C to 850 °C. It was also discovered that after 8 hours of heat treatment at 650 °C, residual stress can be reduced by 76% to 81% (Knowles, Becker & Tait 2012). They also reported that annealing at 950 °C for 1 hour resulted in a residual stress decrease ranging from 94% to 97%.

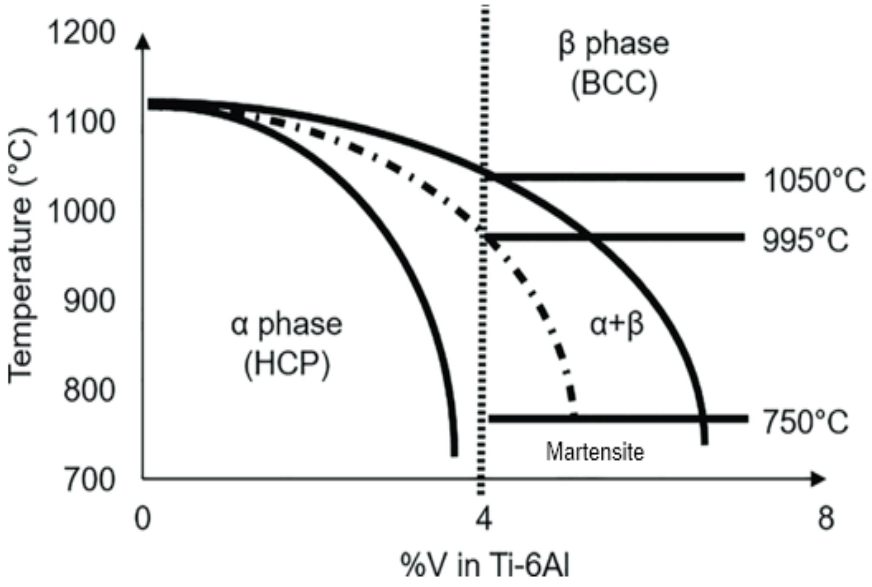

FIGURE 1. Phase diagram of Ti6Al4V accessed through CC BY 4.0 (Majumdar et al. 2019)

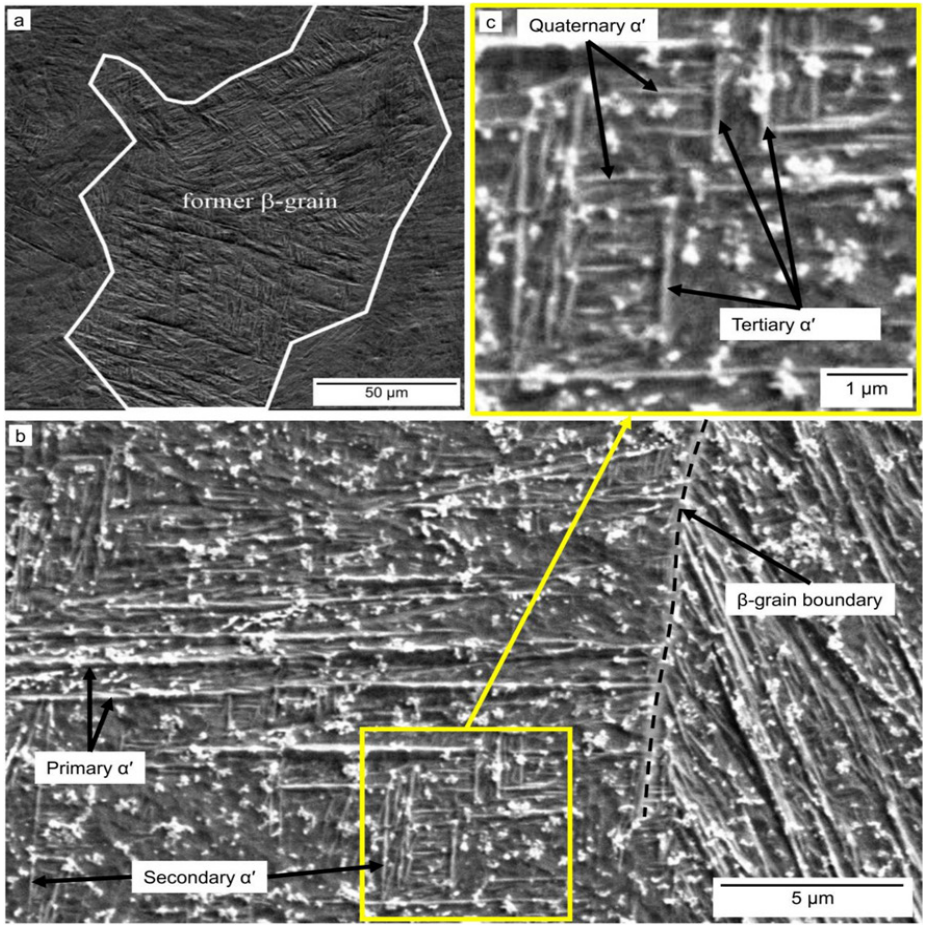

FIGURE 2. Microstructure of LPBF-printed Ti6Al4V that contains: (a) β grain and α' martensite, (b) and (c) four types of α' martensite (Drstvenšek et al. 2021)

TABLE 1. Mechanical properties of LPBF-printed Ti6Al4V before and after heat treatment

Parameters	UTS (MPa)	Yield stress (MPa)	Elongation (%)
(a) Study by Leuders et al. (2013)			
Without heat treatment	1080 ± 30	1008 ± 30	2 ± 2
2 hours at 800 °C	1040 ± 30	962 ± 30	5 ± 2
2 hours at 1050 °C	945 ± 30	798 ± 30	12 ± 2
HIP: 2 hours at 920 °C & 100 MPa	1005 ± 30	912 ± 30	8 ± 2
(b) Study by Kasperovich and Hausmann (2015)			
Without heat treatment	1051	736	12
1 hour at 700 °C	1115	1051	11
2 hours at 900 °C	988	908	10
HIP: 2 hours at 900 °C & 100 MPa	973	885	19
(c) Study by Hosseini and Popovich (2019)			
Without heat treatment	1220 ± 60	1140 ± 60	3.20 ± 1.5
1.5 hours at 950 °C	1083 ± 10	977 ± 35	10.60 ± 1
(d) Study by Wang, Dou and Yang (2018)			
Without heat treatment	1240.50 ± 7.70	-	5.79 ± 0.29
3 hours at 840 °C	1068.30 ± 26.70	-	10.28 ± 0.20

The final microstructure and mechanical properties of LPBF samples are also reported to be influenced by the annealing temperature. Leuders et al. (2013) elaborated that ductility was influenced by grain size and phase fraction, with the growth of β-phase supporting higher elongation, which is achieved through high annealing temperature of 1050 °C. Meanwhile, Kasperovich and Hausmann (2015) reported that a relatively low annealing temperature of 700 °C, can result in the transformation of the fine martensitic microstructure of as-built samples into a coarser α+β grain structure. Also, a higher annealing temperature of 900 °C would produce longer and wider columnar α+β grains. These changes in microstructure contributed to the reduction of strength and ductility observed in heat-treated LPBF samples compared to their as-built counterparts, as detailed in Table 1.

Aside from annealing temperature, holding time is a crucial factor in enhancing ductility (Ter Haar & Becker 2021). Past study concluded that holding times should be longer than 8 hours in order to generate samples with high ductility and little tensile strength loss. While previous studies have demonstrated that heat treatment can effectively reduce residual stress in LPBF-fabricated Ti6Al4V, there remains a lack of studies correlating specific heat treatment parameters with microstructural evolution and mechanical property outcomes. Thus, this preliminary study was conducted to examine the impact of annealing on the microstructure, physical, and mechanical properties of LPBF-fabricated Ti6Al4V.

MATERIALS AND METHODS

SAMPLE PREPARATION

In this study, two Ti6Al4V cubic and six tensile bar samples were printed using Renishaw RenAM 500E LPBF printing machine at default parameters of 200 W laser power, 1200 mm/s scanning speed, 40 µm layer thickness, and 60 µm hatching distance. Ti6Al4V powder used in the printing process, with the size of 21.69 µm - 48.84 µm, was supplied by 3D Gens Sdn. Bhd. (Bukit Jelutong, Selangor, Malaysia). Figure 3 shows the powder morphology and the dimension of as-built cubic and tensile samples. Cubic samples were printed with the dimension of 10 mm × 10 mm × 10 mm, whereas the tensile bar samples printed were in accordance with the ASTM E8/E8M-15a standard. Meanwhile, Table 2 details the chemical composition of the Ti6Al4V powder used in this study. The annealing treatment was done at 935 °C for 8 hours with a heating rate of 5 °C/min and a cooling rate of 0.60 °C/min. For the purpose of this paper, as-built and annealed samples are referred to as AB and HT, respectively.

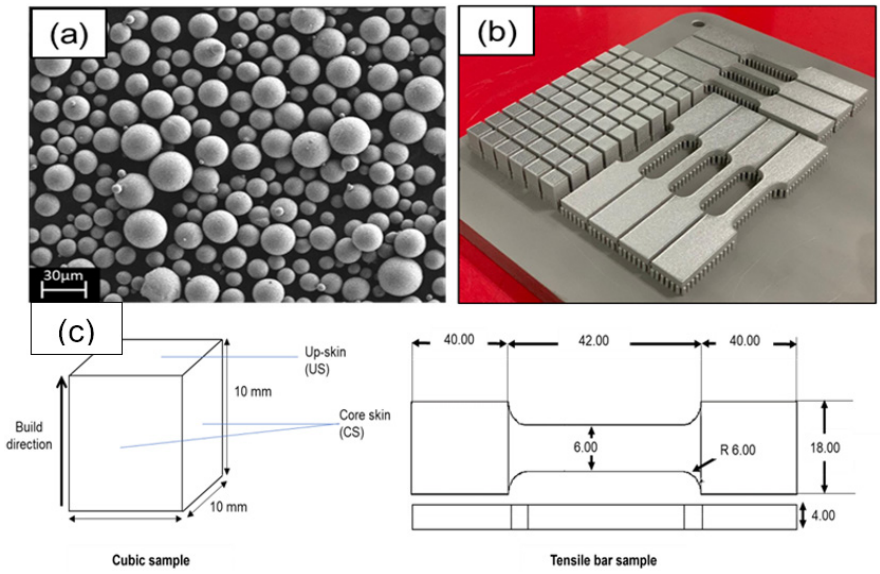

FIGURE 3. (a) Ti6Al4V powder morphology, (b) printed Ti6Al4V cubic and tensile samples on the building platform, and (c) dimension for the cubic and tensile bar samples

TABLE 2. Chemical composition of Ti6Al4V powder used in this study

Element	Ti	Al	V	C	O	N	Fe	H	Others
Percentage (%)	Bal.	5.50 - 6.50	3.50 - 4.50	0.08	0.13	0.03	0.25	0.013	0.40

PHYSICAL TESTS

The physical properties of Ti6Al4V-LPBF samples are compared based on density, surface quality, chemical composition and phase composition. Density of cubic sample was measured through Archimedes' method in accordance with the ASTM B311-17 measurement standards using an electronic weighing machine, Sartorius model BSA224S-CW. Three measurements were taken and averaged using the same cubic sample.

Surface quality was studied based on the surface morphology and surface roughness of samples AB and HT, based on the ASTM F3624 - 23 standards. Surface morphology was observed with a Mitutoyo tabletop microscope and a SEM Hitachi TM1000 machine. Surface roughness was then measured using the Mitutoyo C-3000 surface profiler. Three reading points were measured and averaged with a reading speed of 0.20 mm/s over a reading distance of 3 mm. Meanwhile, the chemical composition of cubic samples was investigated through an EDX analysis using the ZEISS MERLIN SEM machine. The phase composition study was done through an XRD analysis using the Bruker D8 Advance XRD machine.

MECHANICAL TESTS AND MICROSTRUCTURE OBSERVATION

In this study, the mechanical performance of AB and HT was studied through hardness and tensile strength. Hardness was measured using the Micro-Vickers Zwick, ZHVμ machine in accordance with the ASTM E384-11 standard. To test the tensile properties of AB and HT samples, tensile test was done on three tensile bar samples each, using the Exceed Model E64 based on the ASTM-E8/E8M-15a.

For microstructure analysis, sample preparation was done on cubic samples of AB and HT. The samples were ground using silicon carbide (SiC) paper of 300x to 1200x grit and polished with Diamat solutions of 3 μm and 1 μm. The samples were then etched using Keller's reagent for up to 15 s. Microstructure images of AB and HT were captured using a Mitutoyo Optical Microscope (OM). Further microstructure analysis was done by ImageJ software to measure α-phase grain size, with 10 measurements averaged for each sample.

RESULTS AND DISCUSSION

DENSITY

Density measurements showed a slight improvement in the density of Ti6Al4V-LPBF samples through the annealing treatment applied in this study. The density of the HT sample is marginally higher than that of the as-built sample at 4.39 g/cm^3 and 4.37 g/cm^3, respectively. With theoretical density at 4.42 g/cm^3, annealing is capable of maintaining the high density LPBF samples, with HT sample producing 99.28% density. Past studies have reported success in enhancing the density by reducing porosity of LPBF parts after heat treatments such as HIP and annealing (Bassini et al. 2022; Giovagnoli et al. 2021; Gruber et al. 2022). Annealing treatment was reported in previous study to reduce porosity by 13% due to the microstructural transformation from acicular α' into a mixture of α and β phases. This finding is also supported by Su et al. (2022), who attributed the improvement in density to the formation of the α+β phase after heat treatment and the decomposition of acicular α' in as-built samples. The study further elaborated that different ranges in heating temperatures (600 °C to 1000 °C) would either increase or decrease density. This might be due to the phase transformation caused by the temperature changes following the phase diagram of Ti6Al4V.

Annealing treatment applied in this study is in the region of α+β annealing (935 °C) which might have contributed to the slight increase in density observed. Although previous studies reported a significant improvement in density, this study has only recorded a marginal increase in density of 0.46%. The marginal percentage could be attributed to the lack of pre-existent pores in as-built samples produced in this study compared to previous studies. As such, porosity reduction plays a less significant role in density improvement in this study. It is also worth noting that density is principally influenced by LPBF processing parameters as compared to post-processing annealing treatment. Nonetheless, the density obtained in this study both for as-built and heat-treated samples is considered high density with more than 99% relative density parts.

SURFACE QUALITY

In this study, surface roughness for both upskin (US) and core skin (CS) of the samples were studied. Surface profiles using SEM and OM imaging of AB sample can be seen in Figure 4(ai), 4(bi), 4(aiii), 4(biii), while profiles of HT sample can be seen in Figure 4(aii), 4(bii), 4(aiv), 4(biv). Partially melted powder particles adhering to the surface of samples in both AB and HT conditions are identified. The AB sample also exhibits a more prominent scan track and laser path compared to the HT sample. Moreover, the CS surfaces display distinct printing layers, with partially melted particles and balling observed in both samples.

These surface features like balling and partially melted particles have been reported in past study as seen in Figure 5. Aboulkhair et al. (2016) and Shi et al. (2016) both documented the balling phenomenon and partially melted particles appearing on the surface of LPBF-printed surface. These features are attributed to the combination of laser power and scan speed. Improper melting and fusion of powder particles can cause partially melted particles fuse with melt pool, resulting in such features. In contrast, the US profiling of AB and HT samples shows a smooth surface with minimal balling.

Comparing the quality of both type of surfaces, it is apparent that US has a smoother surface. This is supported through surface roughness measurement as seen in Figure 6. As-built samples reported 5.12 μm (US) and 10.48 μm (CS), while heat-treated samples reported slightly higher

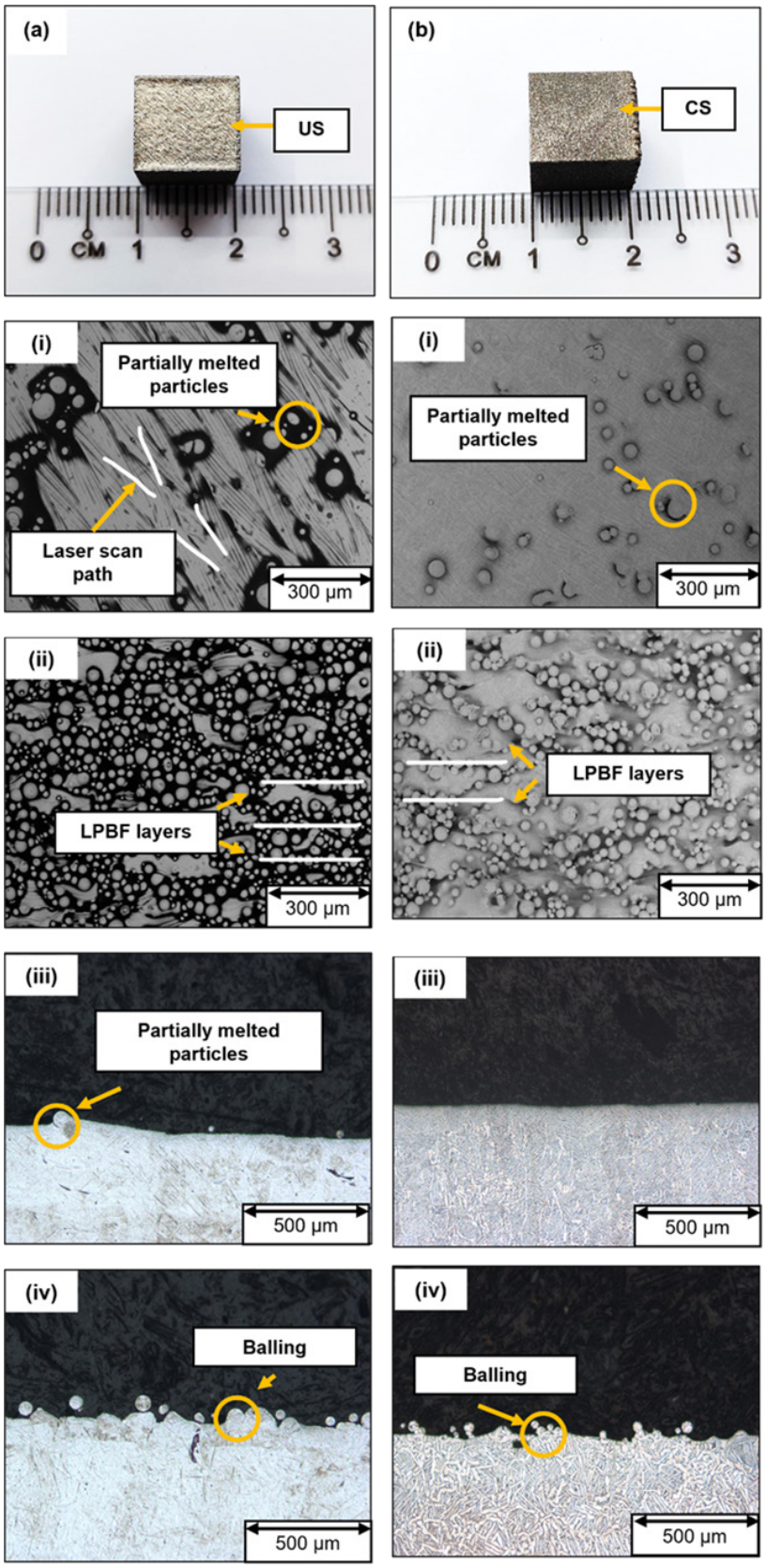

FIGURE 4. Surface profile for (a) upskin (US): SEM images for (i) AB and (ii) HT, and OM images for (iii) AB and (iv) HT; (b) core skin (CS): SEM images for (i) AB and (ii) HT, and OM images for (iii) AB and (iv) HT

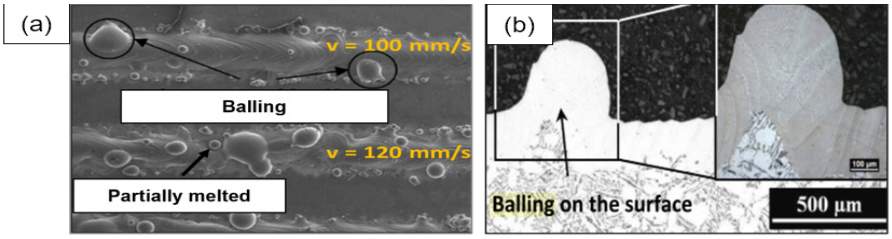

FIGURE 5. Surface features reported in (a) Shi et al. (2016) and (b) Aboulkhair et al. (2016)

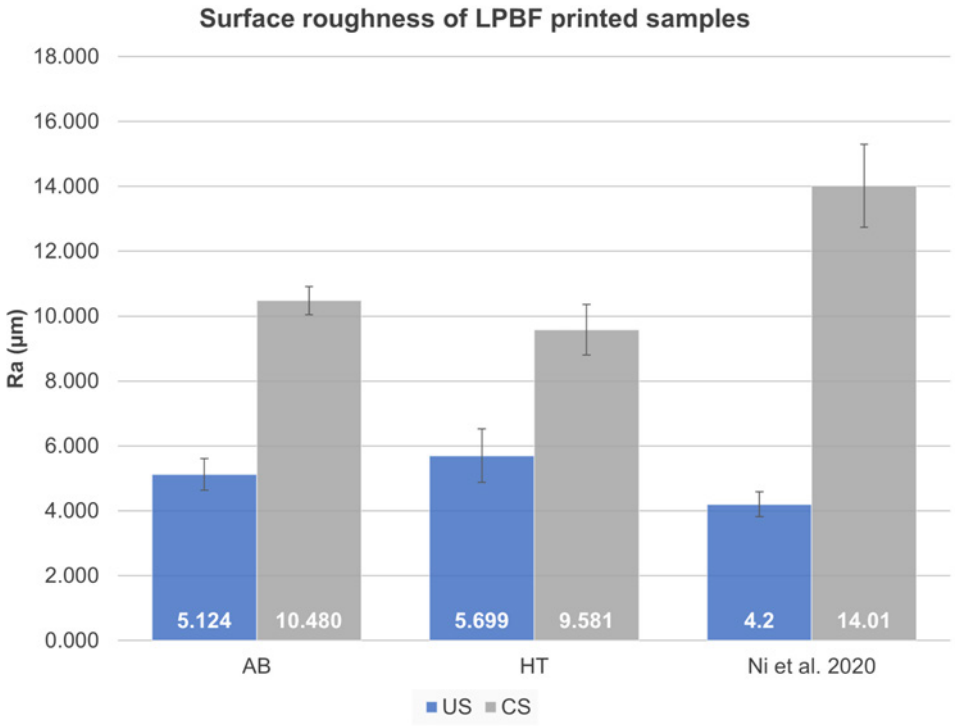

FIGURE 6. Surface roughness result of both upskin (US) and core skin (CS) of AB and HT samples

roughness for US at 5.70 µm and slightly lower value for CS at 9.58 µm. According to past studies, these values are well within the acceptable range (5-40 µm) for LPBF products (Fathin Iliana et al. 2023b; Lee, Nagalingam & Yeo 2021).

The slight variance could be attributed to surface qualities being more influenced by processing parameters than heat treatment at the range of 935 °C for 8 hours employed in this study. Previous reports have found that processing parameters like scanning speed and laser power heavily influence surface roughness (Aripin et al. 2023; Cao et al. 2021; Mazlan et al. 2023). For instance, Wang et al. (2022) concluded that higher energy density resulting from higher laser power, lower scan speed and lower hatching distance would produce lower surface quality with higher surface roughness due to unstable melt pool. The data from the study also showed insignificant difference for surface roughness between as-built samples and heat-treated samples. This highlights the small influence of annealing heat treatment on the surface quality of LPBF-printed Ti6Al4V parts.

PHASE COMPOSITION

XRD analysis in Figure 7 shows that the prominent peaks of Ti6Al4V are evident in all three spectra of Ti6Al4V powder, AB and HT samples. The three main peaks of titanium are identified at angles 35°, 38°, and 41°, corresponding to the respective planes of (100), (002), and (101). These three peaks show the hexagonal close packed (HCP) nature of α-Ti, while the body-centred cubic (BCC) nature of β-Ti is usually detected at angles 39° and 57°, which correspond to planes (110) and (200), respectively. β-Ti is only detected in HT samples due to the annealing

treatment applied, which proves that the beta phase of Ti6Al4V is only stable at high temperature. The rapid cooling and solidification of LPBF in sample AB resulted in predominantly α'-martensite morphology, since most of the beta phase disintegrated into α' owing to beta phase instability at temperatures below β-transus (~980 °C) (Chen et al. 2023). This is further proven since the as-built sample showed no β-peaks. This is similar with the findings of Wang et al. (2016) whereby the presence of β-peaks was detected after annealing treatment at 830 °C over 3 hours was applied and none in as-built sample.

It is worth noting that the crystallinity of alpha phases increased in the as-built and annealed samples when compared to Ti6Al4V powder. The crystal sizes of Ti6Al4V powder in the as-built and annealed samples were also measured and found to be 18.26 nm, 25.21 nm, and 37.86 nm, respectively. Moreover, the change in crystallinity is apparent from the reduced intensity of the peak at (101). In the cyclic melting and solidification of LPBF, some of the β-phase disintegrated to transform into α-phase at temperature ~980 °C, especially at the grain boundary. Rapid rate of cooling and solidification results in a predominantly α' acicular martensite microstructure. For AB sample, α' acicular needle were observed contributing to the increase in crystallinity of alpha phases observed in the XRD spectra. Meanwhile, HT sample has a higher α-phase crystallinity compared to the as-built samples due to the expansion of α+β and the breakdown of acicular α'-martensite after annealing at 935 °C is applied since α' acicular needles are not stable at high temperature.

MICROSTRUCTURE

Figure 8 shows the microstructural changes of Ti6Al4V LPBF samples before and after heat treatment. The LPBF-printed Ti6Al4V sample is seen with microstructure of fully α' martensite needles. Meanwhile, the microstructure of the Ti6Al4V sample after annealing was applied contains a majority of α+β phase. This is due to the annealing heat treatment used is at a temperature higher than the martensite decomposition temperature of 650 °C, the martensite phase changes to a more stable α+β microstructure (Minhalina et al. 2023; Motyka 2021). The changes in microstructure in AB and HT are supported by the XRD analysis, where the small peak β (110) begins to show itself and the intensity of the main peak α (101) decreases.

It can be seen that the fine α' martensite needle in AB samples slowly changing to α phase in HT sample with sizes of 10.10 ± 1.80 μm and 4.70 ± 0.70 μm, for both US and CS, respectively. These large grain sizes can be attributed to the long hour of holding time in this study which is 8 hours. Lekoadi et al. (2021) deduced that long holding time allows the growth and development of grain size. Chen et al. (2024) and Usha Rani et al. (2024) state that the α phase of HT sample will adopt a lamellar or plate-like structures, with increasing thickness depending on the annealing temperature and specific heat treatment regimen. The annealing temperature and holding time also significantly help in increasing the lamellar thickness, thus, enhancing the ductility and fracture toughness of sample (Kerealme et al. 2022). Though, it is important to strike a balance between ductility and strength, as too high of an annealing temperature might cause undesirable interface broadening, which can reduce the mechanical performance.

HARDNESS

Figure 9 depicts the hardness achieved by AB and HT with references from past studies. After annealing, the Ti6Al4V sample decreased by 13.29%, from 414 HV to 359 HV. The decrease may be related to the microstructural changes of Ti6Al4V, as seen in Figure 8. Sample AB has an entirely martensitic microstructure, while sample HT has mostly α+β lamella. The transition from martensite needles to the α+β phase led to a decrease in hardness, since martensite production is necessary for high hardness (Guo et al. 2023; Lekoadi et al 2021). Martensite is created with a high carbon content, which causes a greater dislocation density. A high level of dislocation density is required to achieve high hardness in LPBF products.

TENSILE AND ELONGATION

Figure 10 depicts that while the tensile strength of Ti6Al4V was reduced after heat treatment by 28.17%, elongation has increased drastically by 259% from 3.99% to 14.34%. The drastic increase in the elongation of the heat-treated sample is supported by a study by Hosseini and Popovich (2019). The study reported a 231% improvement in the elongation of the sample was successfully obtained after the sample was heat-treated at 950 °C. Meanwhile, sample AB is seen to have a high UTS value of 1434 MPa due to its completely α' martensite microstructure. A high UTS leads to a low ductility of less than 10%, which does not meet the ASTM F2924-12 standard. Therefore, appropriate heat treatment provides an opportunity to balance tensile strength and ductility by more than 10%.

The AB sample's elongation may be related to the presence of compressive residual stress in the LPBF printed state, which works as a strengthening mechanism by inhibiting crack initiation and propagation. Ter Haar and Becker (2021) found that heat treatment led to significant disintegration of both primary and secondary α. This was identified by the formation and broadening of twin sites where β formed as temperature rises above 900 °C; the breakdown process accelerates due to increased β production. Grain growth rises upon breakdown due to the surface energy attenuation process. Slower cooling rates lead to increased absorption and development of α grain. At high cooling speeds, primary and secondary α grain fragments solidify in the newly created α matrix. The large size of the fragments is highly beneficial in enhancing the ductility of the sample, as the fragment may minimise residual stress caused by the LPBF process (Su et al. 2024).

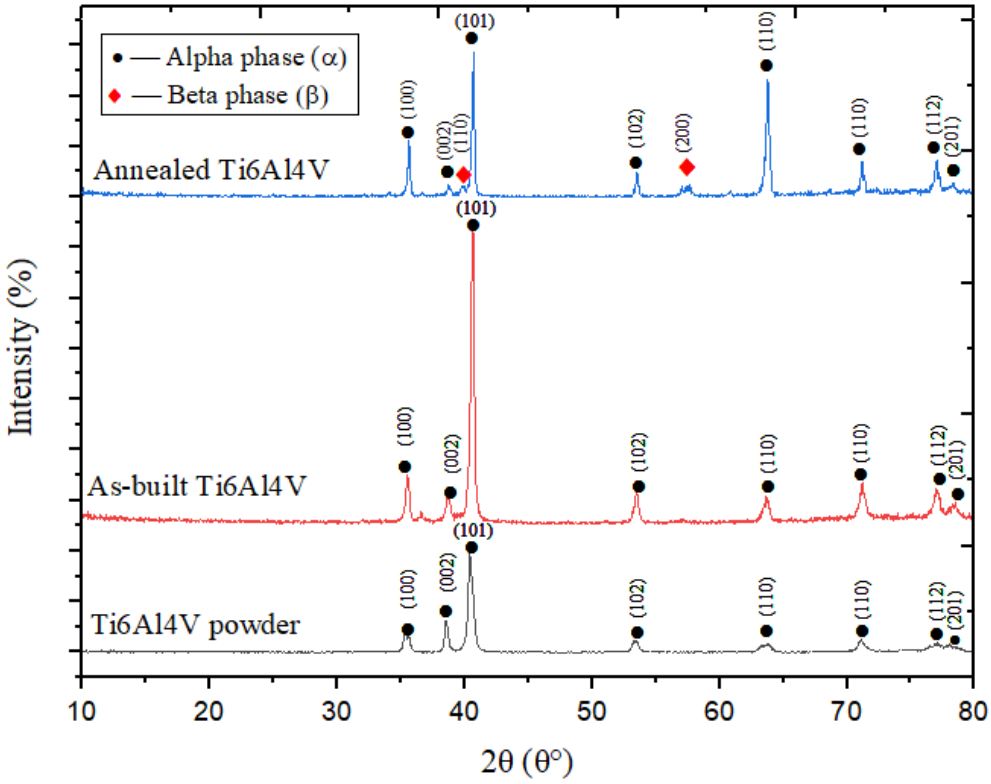

FIGURE 7. XRD analysis for Ti6Al4V powder, AB and HT samples

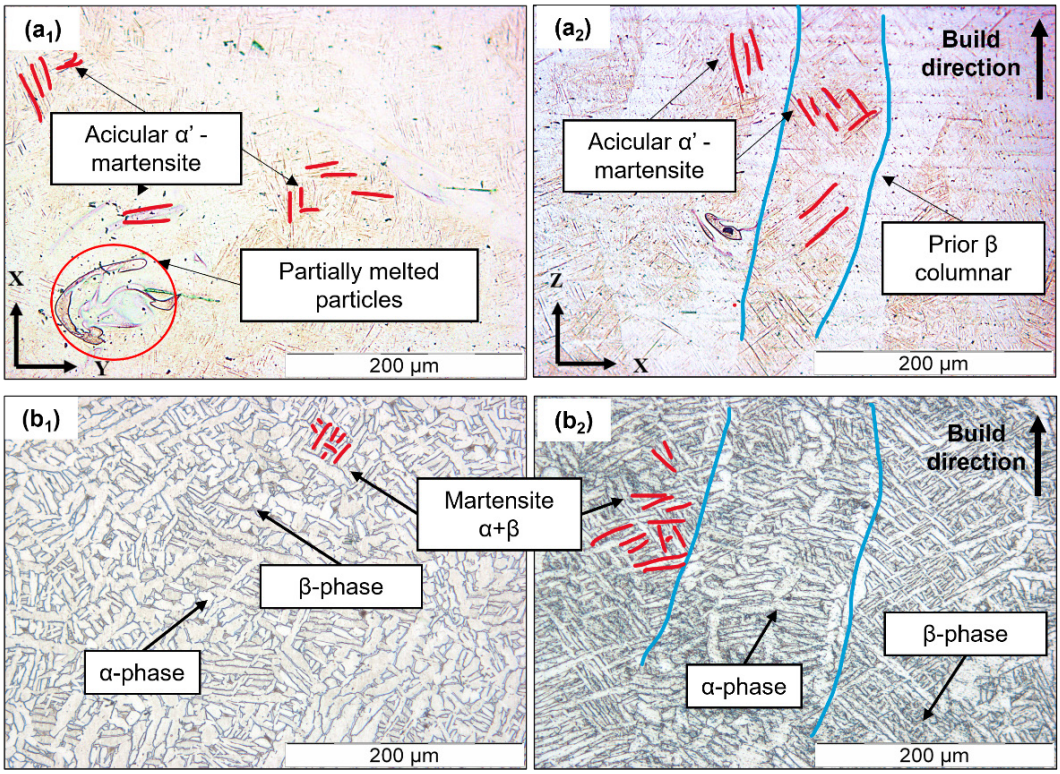

FIGURE 8. Microstructure of (a_1 & a_2) AB and (b_1 & b_2) HT samples

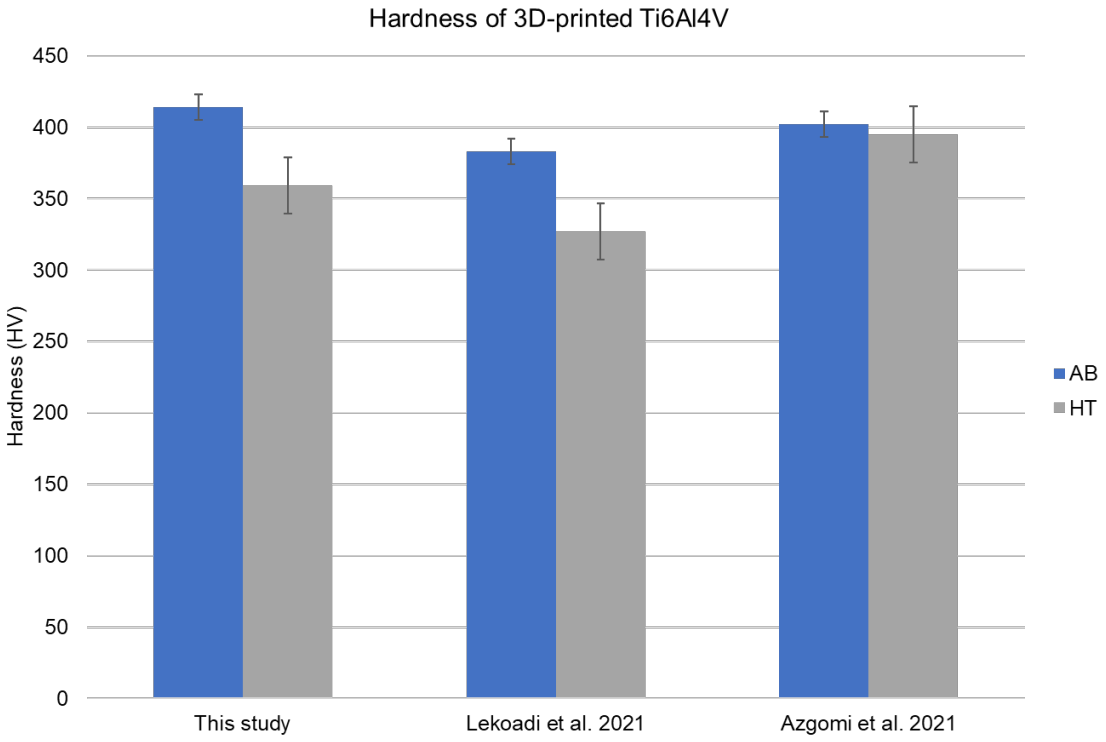

FIGURE 9. Hardness of LPBF Ti6Al4V before and after heat treatment

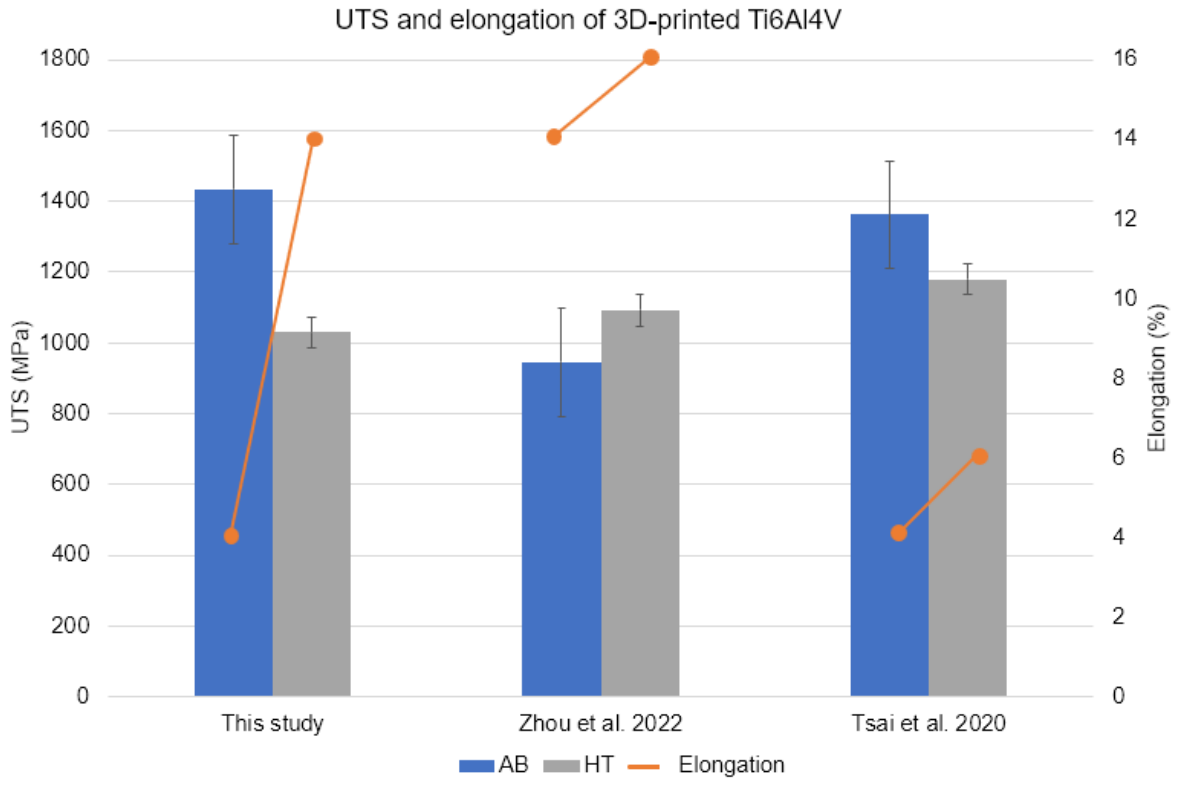

FIGURE 10. Tensile properties of LPBF Ti6Al4V before and after heat treatment

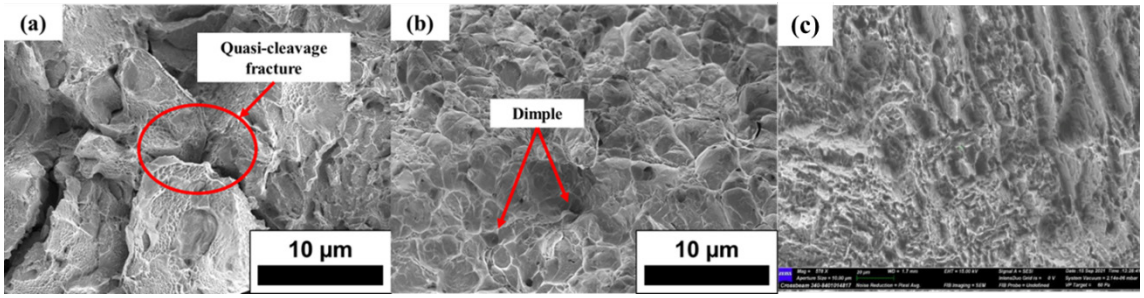

FIGURE 11. Fracture mode of LPBF-fabricated Ti6Al4V (a) before and (b) after heat treatment; (c) dimple fracture found after heat treatment (Lebea et al. 2021)

FRACTURE ANALYSIS

Figure 11 illustrates the types of fracture in the AB and HT samples in which AB sample exhibits both a quasi-cleavage and a dimple fracture mode, HT sample solely contains the latter. According to reports, increasing the cooling rate results in changes in colony size subsequently resulting in an increase in UTS (Ghio & Cerri 2022). At the same time, ductility reaches a peak before rapidly decreasing. At the highest level, the fracture mechanism transitions from ductile transcrystalline dimples to intercrystalline dimples with a continuous α phase layer. However, the UTS value does not change much since the cooling rate has no substantial influence on microstructure change. As a result, a low cooling rate is chosen since it may promote ductility despite a modest decrease in UTS value. As such, this study deduced that apart from reducing the residual stress, heat treatment helps in increasing the ductility of the LPBF-printed Ti6Al4V alloy. Although the hardness and UTS values decrease, it does not have a big impact because the values obtained are still within the standard range. Therefore, all the samples printed for the next study were heat treated through the annealing method after the LPBF process.

CONCLUSIONS

As a preliminary study, this paper has successfully discussed the effects of annealing treatment on the physical, microstructure and mechanical performance of Ti6Al4V-LPBF samples. Based on the findings and discussion, a few key conclusions were highlighted such as the following: a) Heat treatment is effective in producing high-density samples up to 99.27%, while its effects on surface quality is negligible. b) Annealing treatment produces a change in microstructure from acicular α'-martensite into α+β martensite as evident from the microscopic images and XRD analysis. c) Hardness and tensile strength in Ti6Al4V-LPBF are reduced after annealing treatment due to residual stress relief, while the ductility of the samples increases.

ACKNOWLEDGEMENTS

We would like to acknowledge the Ministry of Higher Education (MOHE), Malaysia for funding this study under the Fundamental Research Grant Scheme (FRGS) (FRGS/1/2023/TK10/UKM/02/7).

REFERENCES

Abd-Elaziem, W., Elkatatny, S., Abd-Elaziem, A-E., Khedr, M., Abd El-Baky, M.A., Hassan, M.A., Abu-Okail, M., Mohammed, M., Järvenpää, A., Allam, T. & Hamada, A. 2022. On the current research progress of metallic materials fabricated by laser powder bed fusion process: A review. *Journal of Materials Research and Technology* 20: 681-707.

Aboulkhair, N.T., Maskery, I., Tuck, C., Ashcroft, I. & Everitt, N.M. 2016. Improving the fatigue behaviour of a selectively laser melted aluminium alloy: Influence of heat treatment and surface quality. *Materials & Design* 104: 174-182.

Aripin, M.A., Sajuri, Z., Jamadon, N.H., Baghdadi, A.H., Mohamed, I.F., Syarif, J., Muhammad Aziz, A. & Jamhari, F.I. 2023. Microstructure and mechanical properties of selective laser melted 17–4 PH stainless steel; build direction and heat treatment processes. *Materials Today Communications* 36: 106479.

Azgomi, N., Tetteh, F., Duntu, S.H. & Boakye-Yiadom, S. 2021. Effect of heat treatment on the microstructural evolution and properties of 3D-printed and conventionally produced medical-grade Ti6Al4V ELI alloy. *Metallurgical and Materials Transactions A* 52: 3382-3400.

Bartolomeu, F., Gasik, M., Silva, F.S., Miranda, G. 2022. Mechanical Properties of Ti6Al4V Fabricated by Laser Powder Bed Fusion: A Review Focused on the Processing and Microstructural Parameters Influence on the Final Properties. *Metals* 12: 986. https://doi.org/10.3390/met12060986

Bassini, E., Sivo, A., Martelli, P.A., Rajczak, E., Marchese, G., Calignano, F., Biamino, S. & Ugues, D. 2022. Effects of the solution and first aging treatment applied to as-built and post-HIP CM247 produced via laser powder bed fusion (LPBF). *Journal of Alloys and Compounds* 905: 164213.

Cao, L., Li, J., Hu, J., Liu, H., Wu, Y. & Zhou, Q. 2021. Optimization of surface roughness and dimensional accuracy in LPBF additive manufacturing. *Optics & Laser Technology* 142: 107246.

Chen, J., Fabijanic, D., Brandt, M., Zhao, Y., Ren, S.B. & Xu, W. 2023. Dynamic α globularization in laser powder bed fusion additively manufactured Ti-6Al-4V. *Acta Materialia* 255: 119076.

Chen, Y., Fu, J., Zhou, L., Zhao, Y., Wang, F., Chen, G. & Qin, Y. 2024. Effect of heat treatment on microstructure and mechanical properties of titanium alloy fabricated by laser–arc hybrid additive manufacturing. *Coatings* 14(5): 614.

Drstvenšek, I., Zupanič, F., Bončina, T., Brajlih, T. & Pal, S. 2021. Influence of local heat flow variations on geometrical deflections, microstructure, and tensile properties of Ti-6Al-4 V products in powder bed fusion systems. *Journal of Manufacturing Processes* 65: 382-396.

Fathin Iliana Jamhari, Farhana Mohd Foudzi, Minhalina Ahmad Buhairi, Abu Bakar Sulong, Nabilah Afiqah Mohd Radzuan, Norhamidi Muhamad, Intan Fadhlina Mohamed, Nashrah Hani Jamadon & Kim Seah Tan. 2023a. Influence of heat treatment parameters on microstructure and mechanical performance of titanium alloy in LPBF: A brief review. *Journal of Materials Research and Technology* 24: 4091-4110.

Fathin Iliana Jamhari, Farhana Mohd Foudzi, Minhalina Ahmad Buhairi, Norhamidi Muhamad, Intan Fadhlina Mohamed, Abu Bakar Sulong & Nabilah Afiqah Mohd Radzuan. 2023b. Impact of hot isostatic pressing on surface quality, porosity and performance of Ti6Al4V manufactured by laser powder bed fusion: A brief review. *J. Tribol.* 36: 1-15.

Ghio, E. & Cerri, E. 2022. Additive manufacturing of AlSi10Mg and Ti6Al4V lightweight alloys via laser powder bed fusion: A review of heat treatments effects. *Materials* 15(6): 2047.

Giovagnoli, M., Silvi, G., Merlin, M., Di Giovanni, M.T. 2021. Effect of different heat-treatment routes on the impact properties of an additively manufactured AlSi10Mg alloy. *Materials Science and Engineering: A* 802. doi: 10.1016/j.msea.2020.140671.

Gruber, K., Stopyra, W., Kobiela, K., Madejski, B., Malicki, M. & Kurzynowski, T. 2022. Mechanical properties of Inconel 718 additively manufactured by laser powder bed fusion after industrial high-temperature heat treatment. *Journal of Manufacturing Processes* 73: 642-659.

Guo, S., Li, Y., Gu, J., Liu, J., Peng, Y., Wang, P., Zhou, Q. & Wang, K. 2023. Microstructure and mechanical properties of Ti6Al4V/B4C titanium matrix composite fabricated by selective laser melting (SLM). *Journal of Materials Research and Technology* 23: 1934-1946.

Hosseini, E. & Popovich. V.A. 2019. A review of mechanical properties of additively manufactured Inconel 718. *Additive Manufacturing* 30: 100877.

Kasperovich, G. & Hausmann, J. 2015. Improvement of fatigue resistance and ductility of TiAl6V4 processed by selective laser melting. *Journal of Materials Processing Technology* 220: 202-214.

Kerealme, S., Bai, C., Jia, Q., Xi, T., Zhang, Z., Li, D., Xia, Z., Yang, R. & Yang, K. 2022. Effect of annealing temperature on as-cast Ti6Al4V–5Cu alloy microstructure, tensile properties, and fracture toughness. *Materials Today Communications* 33: 104508.

Knowles, C.R., Becker, T.H. & Tait, R.B. 2012. Residual stress measurements and structural integrity implications for selective laser melted Ti-6Al-4V: General article. *South African Journal of Industrial Engineering* 23(3): 119-129.

Korkmaz, M.E., Gupta, M.K., Waqar, S., Kuntoğlu, M., Krolczyk, G.M., Maruda, R.W. & Pimenov, D.Y. 2022. A short review on thermal treatments of Titanium & Nickel based alloys processed by selective laser melting. *Journal of Materials Research and Technology* 16: 1090-1101.

Kruth, J-P., Deckers, J., Yasa, E. & Wauthlé, R. 2012. Assessing and comparing influencing factors of residual stresses in selective laser melting using a novel analysis method. *Proceedings of the Institution of Mechanical Engineers, Part B: Journal of Engineering Manufacture* 226(6): 980-991.

Lebea, L., Ngwangwa, H.M., Desai, D. & Nemavhola, F. 2021. Experimental investigation into the effect of surface roughness and mechanical properties of 3D-printed titanium Ti-64 ELI after heat treatment. *International Journal of Mechanical and Materials Engineering* 16: 16.

Lee, J-Y., Nagalingam, A.P. & Yeo, S.H. 2021. A review on the state-of-the-art of surface finishing processes and related ISO/ASTM standards for metal additive manufactured components. *Virtual and Physical Prototyping* 16(1): 68-96.

Lee, W., Hyun, Y.T., Won, J.W. & Yoon, J. 2024. Numerical simulation for β/α transformation of Ti–6Al–4V alloy using a lattice Boltzmann - Cellular automata method. *Journal of Materials Research and Technology* 32: 1416-1425.

Lekoadi, P., Tlotleng, M., Annan, K., Maledi, N. & Masina, B. 2021. Evaluation of heat treatment parameters on microstructure and hardness properties of high-speed selective laser melted Ti6Al4V. *Metals* 11(2): 255.

Leuders, S., Thöne, M., Riemer, A., Niendorf, T., Tröster, T., Richard, H.A. & Maier, H.J. 2013. On the mechanical behaviour of titanium alloy TiAl6V4 manufactured by selective laser melting: Fatigue resistance and crack growth performance. *International Journal of Fatigue* 48: 300-307.

Majumdar, T., Bazin, T., Massahud Carvalho Ribeiro, E., Frith, J.E. & Birbilis, N. 2019. Understanding the effects of PBF process parameter interplay on Ti-6Al-4V surface properties. *PLoS ONE* 14(8): e0221198.

Mazeeva, A., Masaylo, D., Konov, G. & Popovich, A. 2024. Multi-metal additive manufacturing by extrusion-based 3D printing for structural applications: A review. *Metals* 14(11): 1296.

Mazlan, M.R., Jamadon, N.H., Rajabi, A., Sulong, A.B., Mohamed, I.F., Yusof, F. & Jamal, N.A. 2023. Necking mechanism under various sintering process parameters - A review. *Journal of Materials Research and Technology* 23: 2189-2201.

Minhalina Ahmad Buhairi, Farhana Mohd Foudzi, Fathin Iliana Jamhari, Abu Bakar Sulong, Nabilah Afiqah Mohd Radzuan, Norhamidi Muhamad, Intan Fadhlina Mohamed, Abdul Hadi Azman, Wan Sharuzi Wan Harun & Al-Furjan, M.S.H. 2023. Review on volumetric energy density: Influence on morphology and mechanical properties of Ti6Al4V manufactured via laser powder bed fusion. *Progress in Additive Manufacturing* 8(2): 265-283.

Motyka, M. 2021. Martensite formation and decomposition during traditional and AM processing of two-phase titanium alloys - An overview. *Metals* 11(3): 481.

Narasimharaju, S.R., Zeng, W., See, T.L., Zhu, Z., Scott, P., Jiang, X. & Lou, S. 2022. A comprehensive review on laser powder bed fusion of steels: Processing, microstructure, defects and control methods, mechanical properties, current challenges and future trends. *Journal of Manufacturing Processes* 75: 375-414.

Ni, C., Zhu, L., Zheng, Z., Zhang, J., Yang, Y., Yang, J., Bai, Y., Weng, C., Lu, W.F. & Wang, H. 2020. Effect of material anisotropy on ultra-precision machining of Ti-6Al-4V alloy fabricated by selective laser melting. *Journal of Alloys and Compounds* 848: 156457.

Pal, S., Bončina, T., Lojen, G., Brajlih, T., Fabjan, E.Š., Gubeljak, N., Finšgar, M. & Drstvenšek, I. 2024. Fine martensite and beta-grain variational effects on mechanical properties of Ti–6Al–4V while laser parameters change in laser powder bed fusion. *Materials Science and Engineering: A* 892: 146052.

Shi, X., Ma, S., Liu, C., Chen, C., Wu, Q., Chen, X. & Lu, J. 2016. Performance of high layer thickness in selective laser melting of Ti6Al4V. *Materials* 9(12): 975.

Su, G., Chang, J., Zhai, Z., Wu, Y., Ma, Y., Yang, R. & Zhang, Z. 2024. On the role of grain morphology in the mechanical behavior of laser powder bed fusion metastable β titanium alloy. *Materials Science and Engineering: A* 909: 146844.

Su, J., Jiang, F., Li, J., Tan, C., Xu, Z., Xie, H., Liu, J., Tang, J., Fu, D., Zhang, H. & Teng, J. 2022. Phase transformation mechanisms, microstructural characteristics and mechanical performances of an additively manufactured Ti-6Al-4V alloy under dual-stage heat treatment. *Materials & Design* 223: 111240.

Ter Haar, G.M. & Becker, T.H. 2021. Low temperature stress relief and martensitic decomposition in selective laser melting produced Ti6Al4V. *Material Design & Processing Communications* 3(1): e138.

Tsai, M-T., Chen, Y-W., Chao, C-Y., Jang, J.S.C., Tsai, C-C., Su, Y-L. & Kuo, C-N. 2020. Heat-treatment effects on mechanical properties and microstructure evolution of Ti-6Al-4V alloy fabricated by laser powder bed fusion. *Journal of Alloys and Compounds* 816: 152615.

Usha Rani, S., Sadhasivam, M., Kesavan, D., Pradeep, K.G. & Kamaraj, M. 2024. A multi-scale microscopic study of phase transformations and concomitant α/β interface evolution in additively manufactured Ti-6Al-4V alloy. *Materials Science and Engineering: A* 900: 146400.

Wang, D., Dou, W. & Yang, Y. 2018. Research on selective laser melting of Ti6Al4V: Surface morphologies, optimized processing zone, and ductility improvement mechanism. *Metals* 8(7): 471.

Wang, M., Wu, Y., Lu, S., Chen, T., Zhao, Y., Chen, H. & Tang, Z. 2016. Fabrication and characterization of selective laser melting printed Ti–6Al–4V alloys subjected to heat treatment for customized implants design. *Progress in Natural Science: Materials International* 26(6): 671-677.

Wang, Y., Yang, G., Zhou, S., Sun, C., Li, B., An, D., Zhang, S. & Xiu, S. 2022. Effect of laser remelting on microstructure and mechanical properties of Ti–6Al–4V alloy prepared by inside-beam powder feeding. *Materials Science and Engineering: A* 861: 144266.

Zhou, Y., Wang, K., Sun, Z. & Xin, R. 2022. Simultaneous improvement of strength and elongation of laser melting deposited Ti-6Al-4V titanium alloy through three-stage heat treatment. *Journal of Materials Processing Technology* 306: 117607.

*Corresponding author; email: farhana.foudzi@ukm.edu.my